

Electronic Supporting Information

The water, of course! Impurity-induced polymorphism in the self-assembly of interfacial trimesic acid monolayers

Manuela Hocke, Natalia Martsinovich, and Markus Lackinger

Materials and Methods

STM experiments were carried out with a home-built ambient instrument with an integrated linear stick-slip nano-positioner for the coarse approach. The STM was operated using a SPM 100 control electronics from RHK, and mechanically cut PtIr (90/10) tips were used for imaging. The typical tunneling parameters were used, with voltages ranging from 500 to 1200 mV and currents ranging from 30 to 60 pA. Highly Oriented Pyrolytic Graphite (HOPG, grade ZYB, Optigraph GmbH) samples were cleaved with adhesive tape prior to each experiment. Trimesic acid (Merck, $\geq 95\%$), heptanoic acid (TCI, 98% and Merck, $\geq 99\%$) and hexanoic acid (TCI, 98%) were acquired from commercial suppliers with purities as indicated. Double distilled medical-grade H₂O was used for the solvent wetting experiments.

UV-Vis absorption spectroscopy was performed using a USB 4000 spectrometer from Ocean Optics, equipped with a DH-Mini-Deuterium-Halogen light source. A quartz glass cuvette with 1 mm optical path length (Helma) was used, and pure solvent from the same batch served as the reference.

Vacuum distillation was carried out using a standard setup. The heptanoic acid solvent was held in a 250 mL round-bottom distillation flask, which was heated in a stirred oil bath on a temperature-controlled hot plate. A vacuum distillation head with a thermometer directed the vapor from the distillation flask to a downward-oriented, water-cooled Liebig condenser. This led directly into a distillation distribution adapter, which allowed the distillate to be collected in freely selectable 100 mL round-bottom receiving flasks. The distillation setup was evacuated using a rotary vane pump protected by a liquid nitrogen cold trap. The pressure typically remained below 1.6×10^{-1} mbar, as measured with a Pirani gauge directly at the vacuum pump. In a typical distillation, the temperature of the oil bath was around 120 °C - 140 °C, while the measured temperature of the heptanoic acid vapor was in the range 90 °C - 100 °C. The first few millilitres of the distillate were always discarded.

***Ab initio* Molecular Dynamics calculations**

Ab initio Molecular Dynamics (AIMD) calculations were carried out using Density Functional Theory (DFT) as implemented in the SIESTA software package,^{1, 2} using the PBE functional³ with the D2 dispersion correction.⁴ The graphite surface was represented by either single-layer or bilayer graphene, with a rectangular unit cell (dimensions $21.30 \times 9.84 \text{ \AA}$) obtained by $5 \times 4 \times 1$ or $5 \times 4 \times 2$ extension of the rectangular 4-atom graphene unit cell. The system size was chosen to leave approximately 6 \AA space around the adsorbates. To avoid interference with unbound carboxylic acid groups and reduce system size, a hydrogen-bonded benzoic acid dimer was used instead of a TMA dimer. Several AIMD runs were performed on both single-layer and bilayer graphene, with the water molecule starting from different positions above the hydrogen bonds of the benzoic acid dimer. The AIMD calculations were performed in the NVT ensemble, with a temperature of 298 K maintained using the Nose-Hoover thermostat. Each time step was 1.0 fs, with simulation times up to 1.5 ps (on bilayer graphene) and 4 ps (on single-layer graphene).

Additional STM data

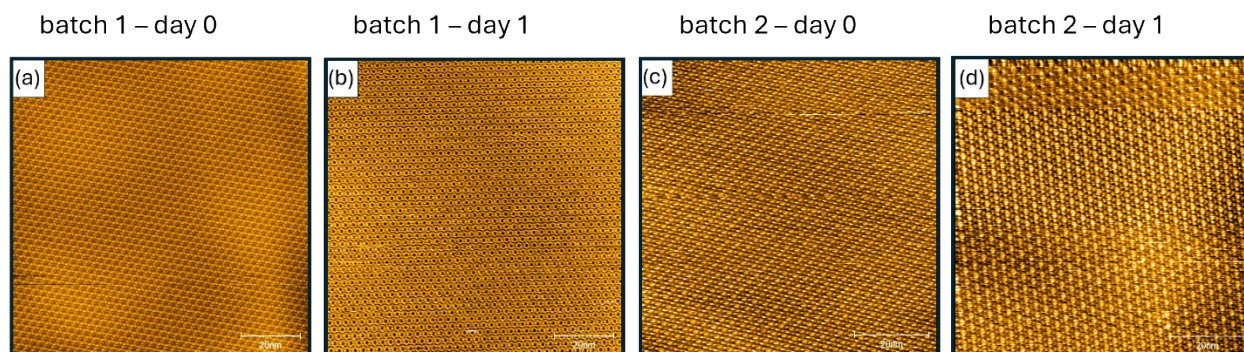


Fig. S1 Phase purity of unexpectedly observed FL polymorph. Large-scale STM images acquired from saturated TMA solutions, prepared as follows: (a) and (c) immediately after the respective 7A bottle was opened and (b) and (d) prepared again on the following day. 7A solvents were used from two different batches. In all cases, at least three macroscopically distinct spots on the samples were probed, with the FL polymorph exclusively observed. Although individual TMA molecules cannot be discerned at this scale, and the observed STM contrast can vary, the significant difference in lattice parameters between the CW ($a = b = 1.65$ nm) and FL ($a = b = 2.60$ nm) polymorphs allows for unambiguous identification. Additionally, only the CW polymorph exhibits a distinctive Moiré pattern which can be clearly recognized even at lower magnification (cf. Fig. S2).

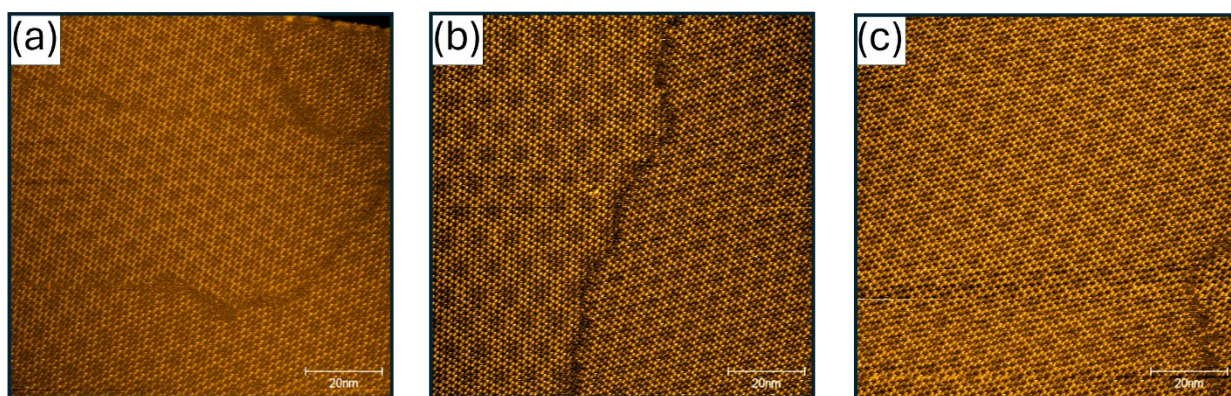


Fig. S2 TMA self-assembly from 6A-contaminated 7A solvent. STM images of TMA monolayers self-assembled from a saturated solution prepared with 1:10 (v/v) mixture of 6A and 7A solvents; (a) – (c) acquired from macroscopically different locations on the same sample. Pure 6A solvent reliably yields the FL polymorph.⁵ However, even at this unrealistically high concentration of 6A “impurities” in the 7A solvent, only the CW polymorph is observed. This allows us to safely exclude the possibility that 6A contamination of the 7A solvent is responsible for the emergence of the FL polymorph.

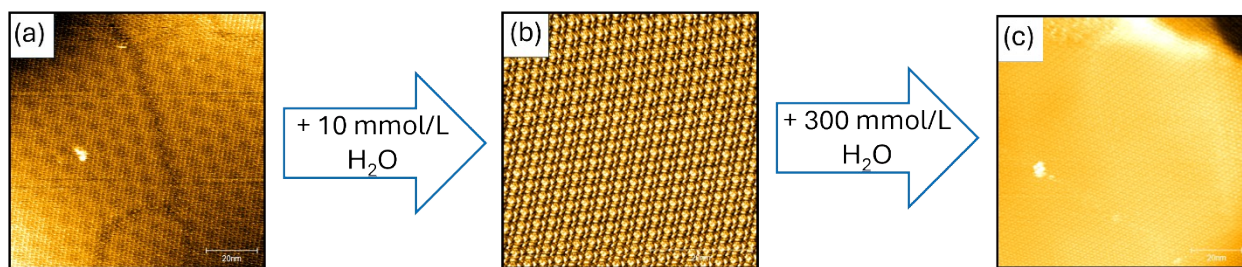


Fig. S3 TMA polymorph control by adding liquid water. STM images acquired (a) from the initial TMA solution, which afforded only the CW polymorph; (b) after adding 10 mmol/L of liquid water to the 7A solvent, resulting in the emergence of first FL domains (shown here); (c) after consecutively increasing the concentration of added water to 300 mmol/L. The FL polymorph was almost exclusively observed, with scattered smaller CW domains, while the reference solution continues to show the CW polymorph.

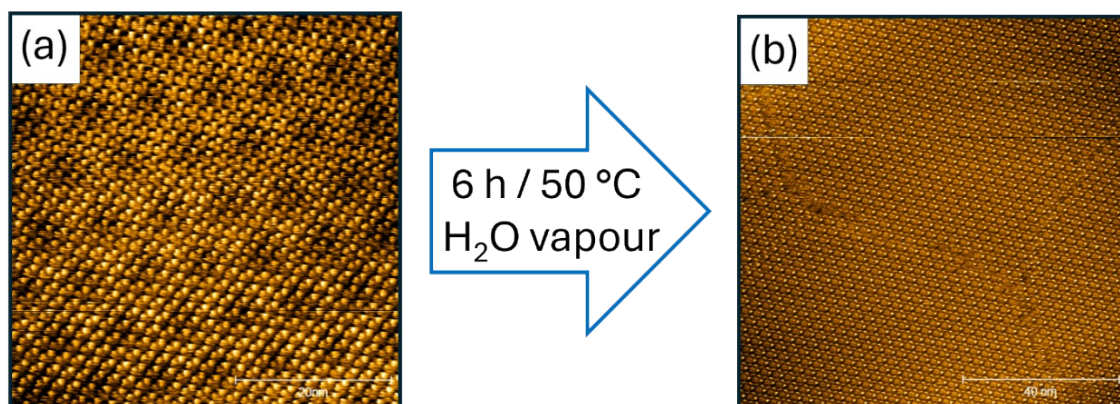


Fig. S4 TMA polymorph control by solvent exposure to water vapour. STM images acquired (a) from the initial TMA solution, which afforded only the CW polymorph; (b) after exposure of the 7A solvent to saturated water vapour at 50 °C for ~6 h (see Fig. S13(c) for experimental setup). Exclusively the FL polymorph was observed in this experiment; however, other analogous experiments still resulted in the CW polymorph.

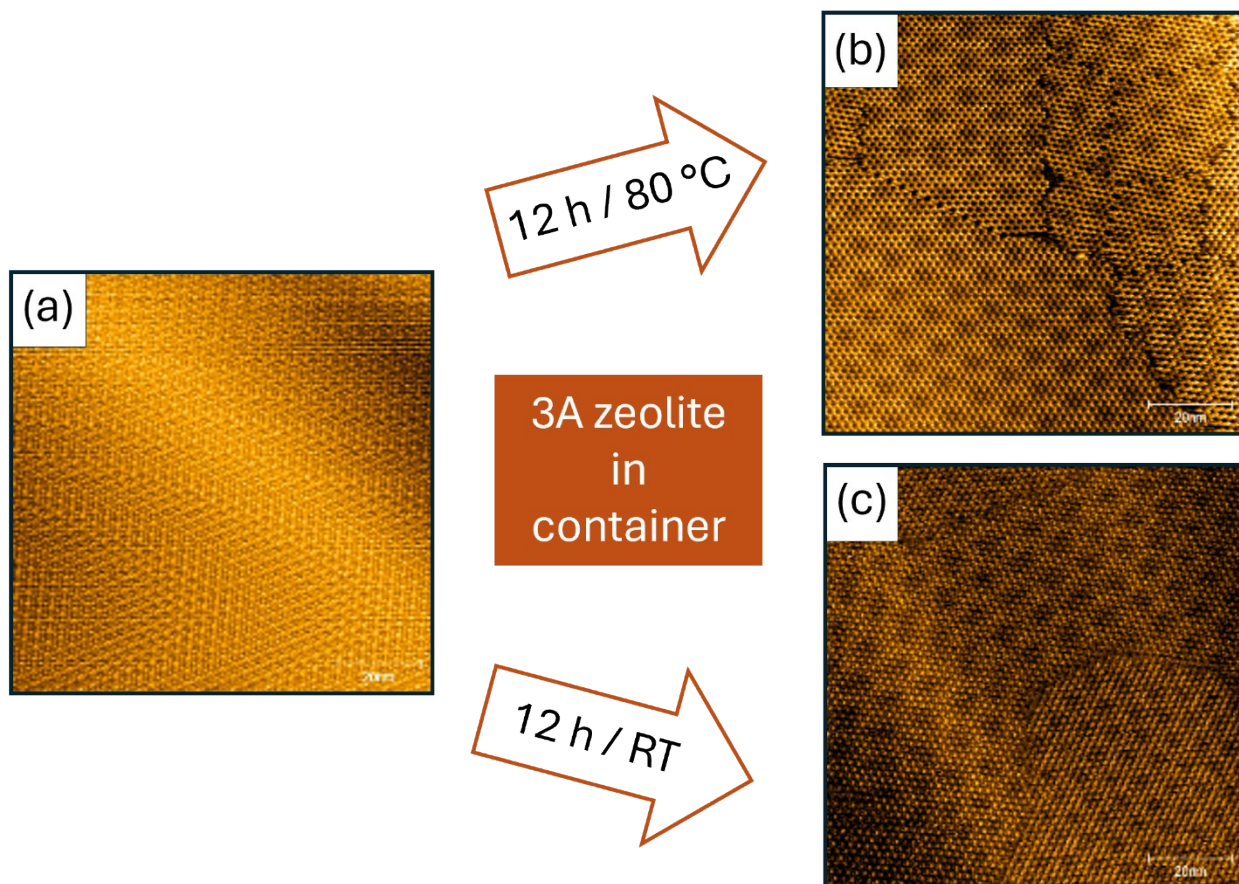


Fig. S5 TMA polymorph control by drying the wetted 7A solvent with 3A zeolite. STM images acquired: (a) of the TMA solution prepared with artificially wetted 7A solvent, which yielded only the FL polymorph; after exposing the solution to 3A zeolite (b) at an elevated temperature of 80 °C and (c) at room temperature (RT) for 12 h (see Fig. S13(a) for the experimental setup). Irrespective of heating, a complete structural change from FL to CW was observed in both cases.

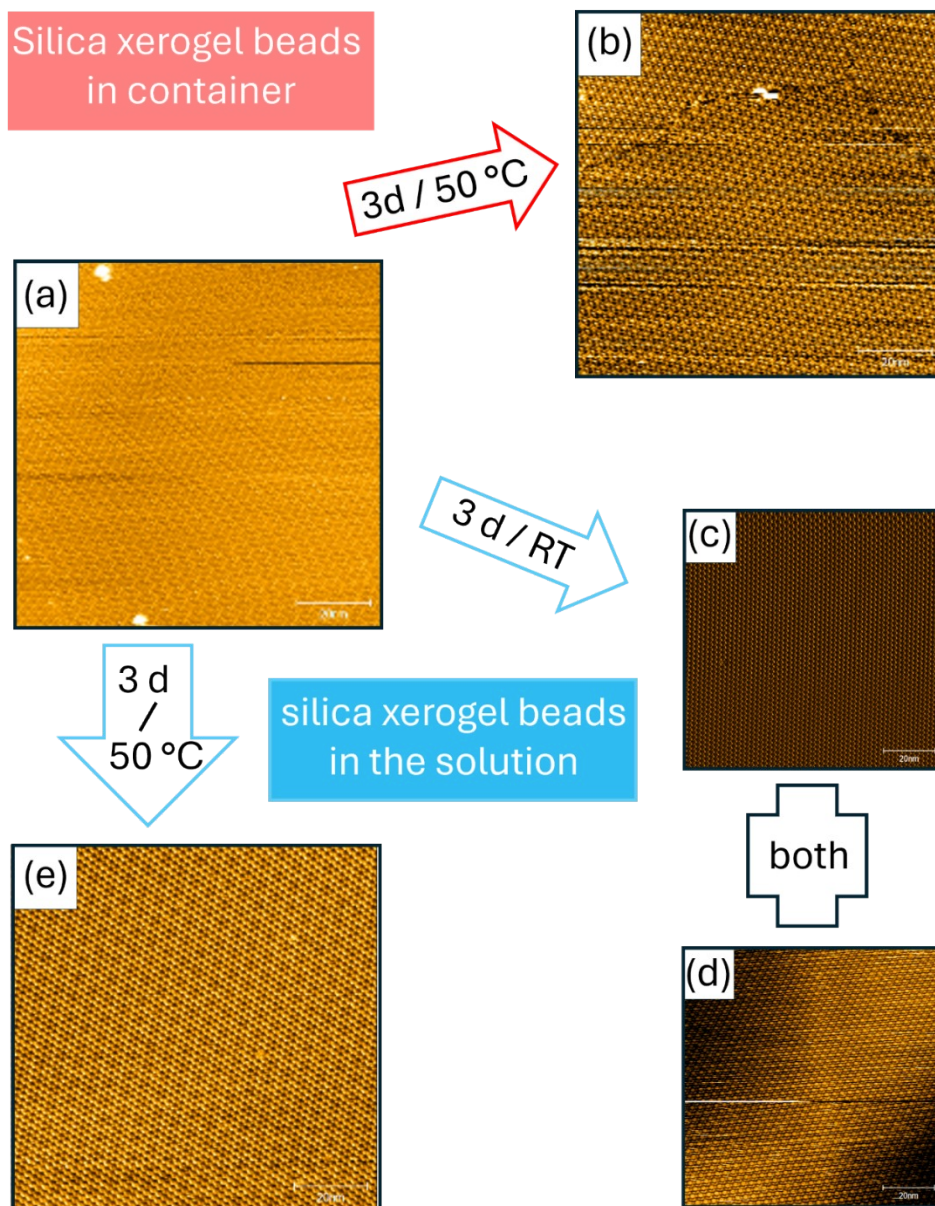


Fig. S6 Polymorph control by drying the wetted 7A solvent with silica xerogel beads. STM images acquired (a) of the TMA solution prepared with artificially wetted 7A solvent, which yielded only the FL polymorph; (b) after heating the TMA solution for 3 days in a closed container with silica xerogel beads present (see Fig. S13(b) for the experimental setup). (c) – (e) after immersing the silica xerogel beads into 7A solvent for 3 days (c) / (d) at room temperature and (e) at an elevated temperature of 50 °C. The presence of silica xerogel beads in the same container as the solvent was not enough to alter the polymorph. However, immersing the silica xerogel beads in solution at room temperature could result in first domains of the CW polymorph co-existing with the initial FL polymorph. In contrast, a complete structural change to the CW polymorph required additional heating. In this case, however, some areas of the graphite were not covered with TMA monolayers (cf. Fig. S7), whereas normally the entire surface is completely covered. This anomaly is tentatively attributed to surface contamination caused by prolonged exposure to silica xerogel beads.

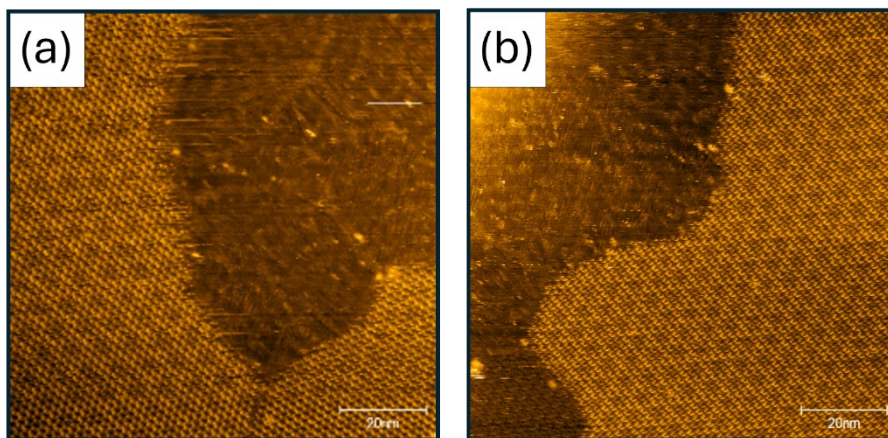


Fig. S7 TMA self-assembly from a solution dried with silica xerogel beads. (a) / (b) STM images acquired from a solution prepared with 7A solvent that was first artificially wetted and subsequently dried by direct immersion of silica xerogel beads and heating to 50 °C for 3 days. The results of two separate experimental runs are shown here. Although emergence of the CW polymorph indicated successful drying of the solvent, some areas appeared empty (darker) with fuzzy contrast. As this observation is unique to the silica xerogel dried samples, it is tentatively assigned with surface contamination.

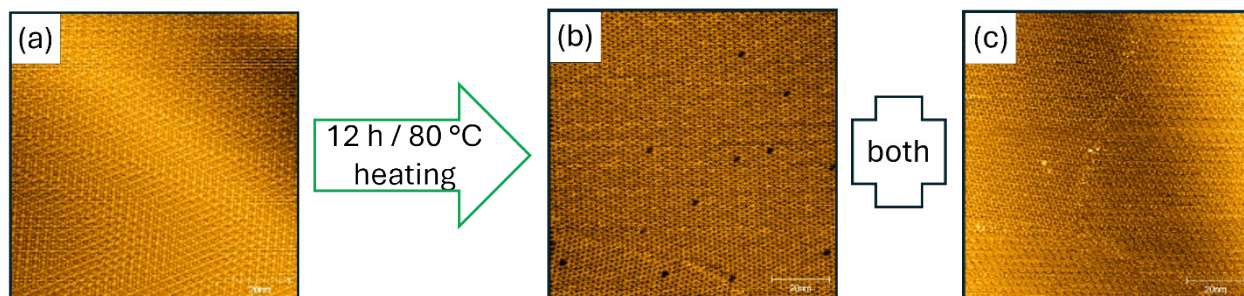


Fig. S8 TMA polymorph control by drying the wetted 7A solvent through heating only. STM images acquired (a) of the TMA solution prepared with artificially wetted 7A solvent, which yielded only the FL polymorph, and (b) / (c) after simply heating the solution at 80 °C for 12 h. In this case, both (b) the CW and (c) FL polymorphs were observed to coexist in macroscopically distinct areas of the sample.

Gas Chromatography-Mass Spectrometry (GC-MS)

The chromatography column used was highly moisture-sensitive, and all samples were dried prior by immersing anhydrous MgSO_4 . Accordingly, these GC-MS analysis does not allow any statement about the water content.

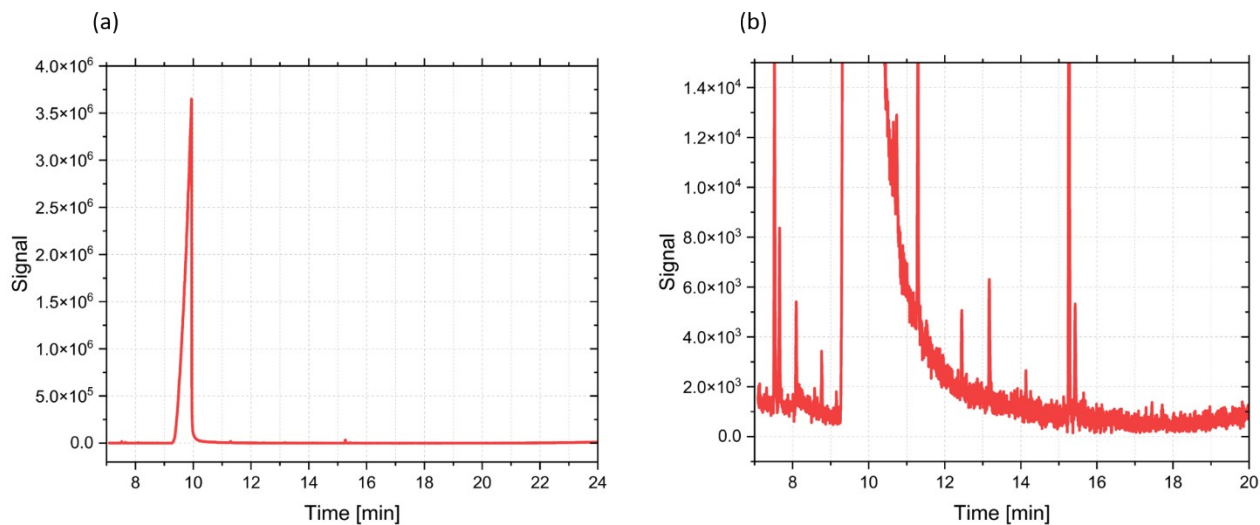


Fig. S9 Exemplary GC-MS chromatogram of one of the 7A solvents used (supplied by Merck). (a) Overview showing the main 7A peak at a retention time of 9.9 min. (b) Enlarged view of the major impurity peaks. These peaks are approximately 150 times smaller than the main 7A peak, and their total amount is consistent with the specified overall purity of $\geq 99\%$.

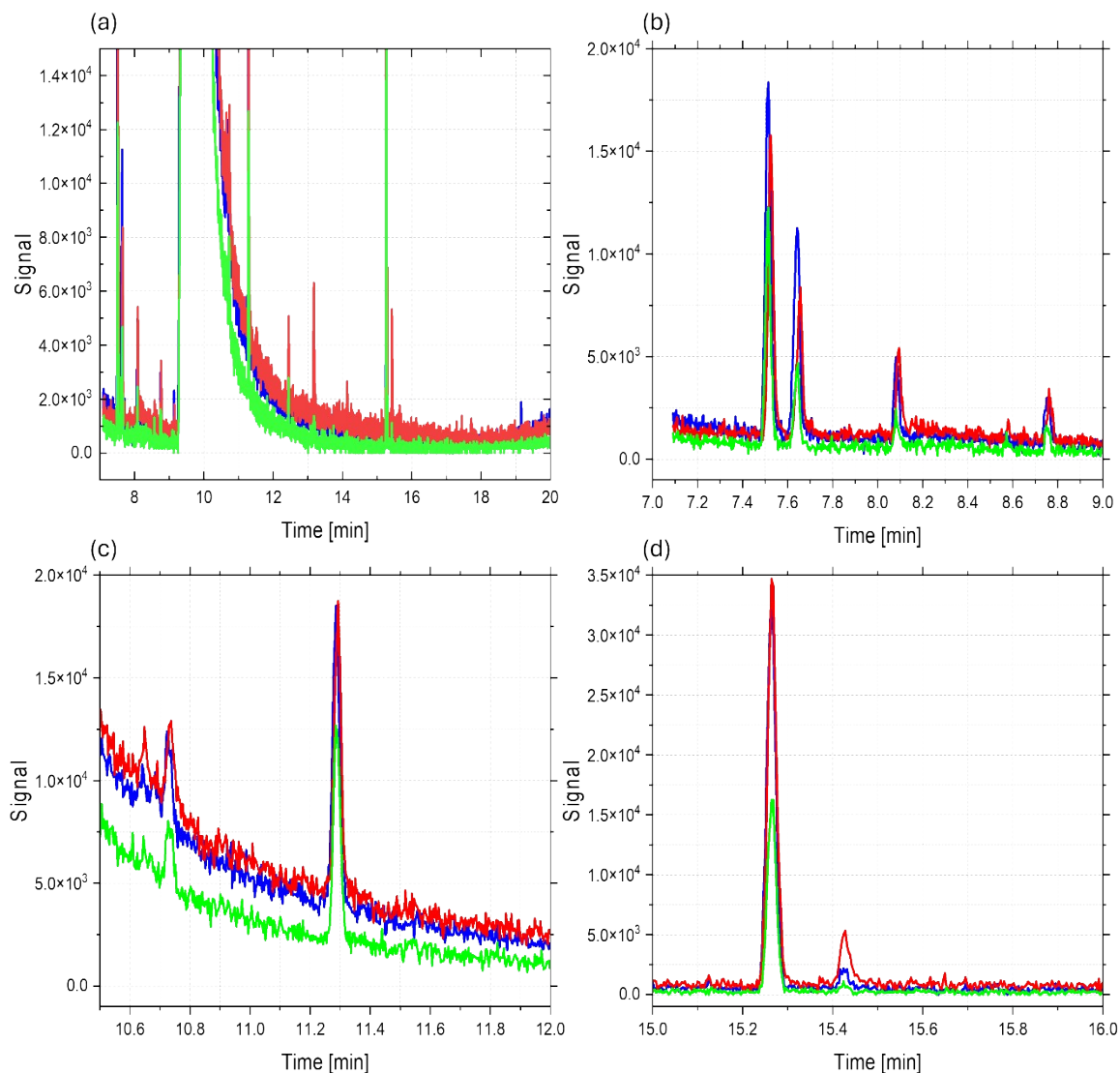


Fig. S10 Comparison of the GC-MS chromatograms of three different 7A solvents from different suppliers and batches: blue (TCI, ~ 1 year old); red (Merck); green (TCI); (the respective suppliers are listed in parentheses). The latter two solvents were acquired around the same time. (a) Overview chromatogram with the main 7A peak at a retention time of 9.9 min cut off. (b) – (d) Close-ups for the retention time regions where main impurity peaks occurred. The chromatograms of all three 7A solvents are surprisingly similar. Additionally, minor deviations in peak position and height could be explained by slight variations in pressure and gas flow between individual GC-MS measurements.

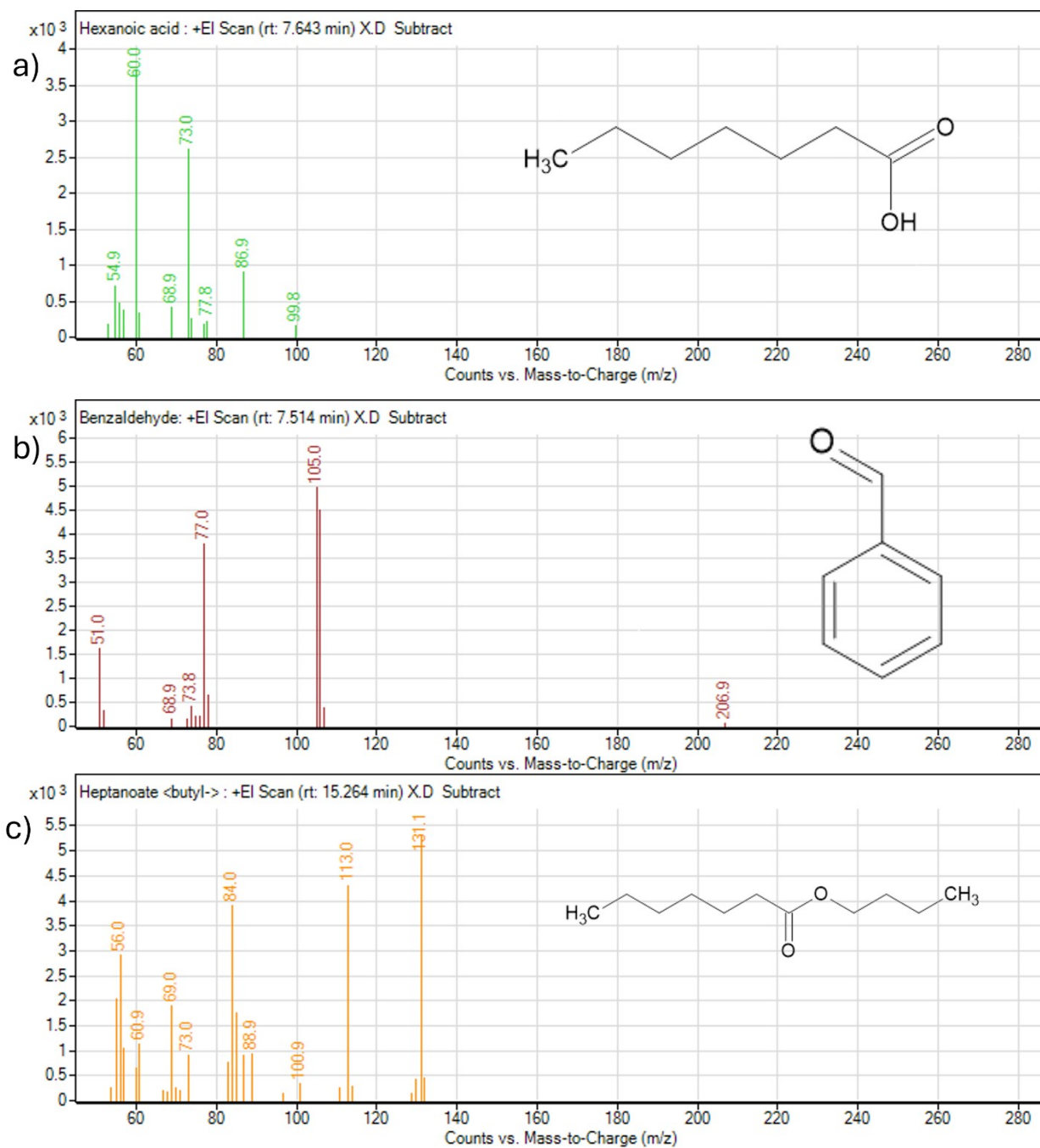


Fig. S11 Corresponding mass spectra (electron ionization) to selected major impurity peaks of the GC-MS chromatogram in Fig. S10. The respective retention times (rt) are indicated on the top left. The following impurities were assigned based on their mass spectra: (a) hexanoic acid, (b) benzaldehyde, (c) butyl heptanoate. Their chemical structures are depicted on the right.

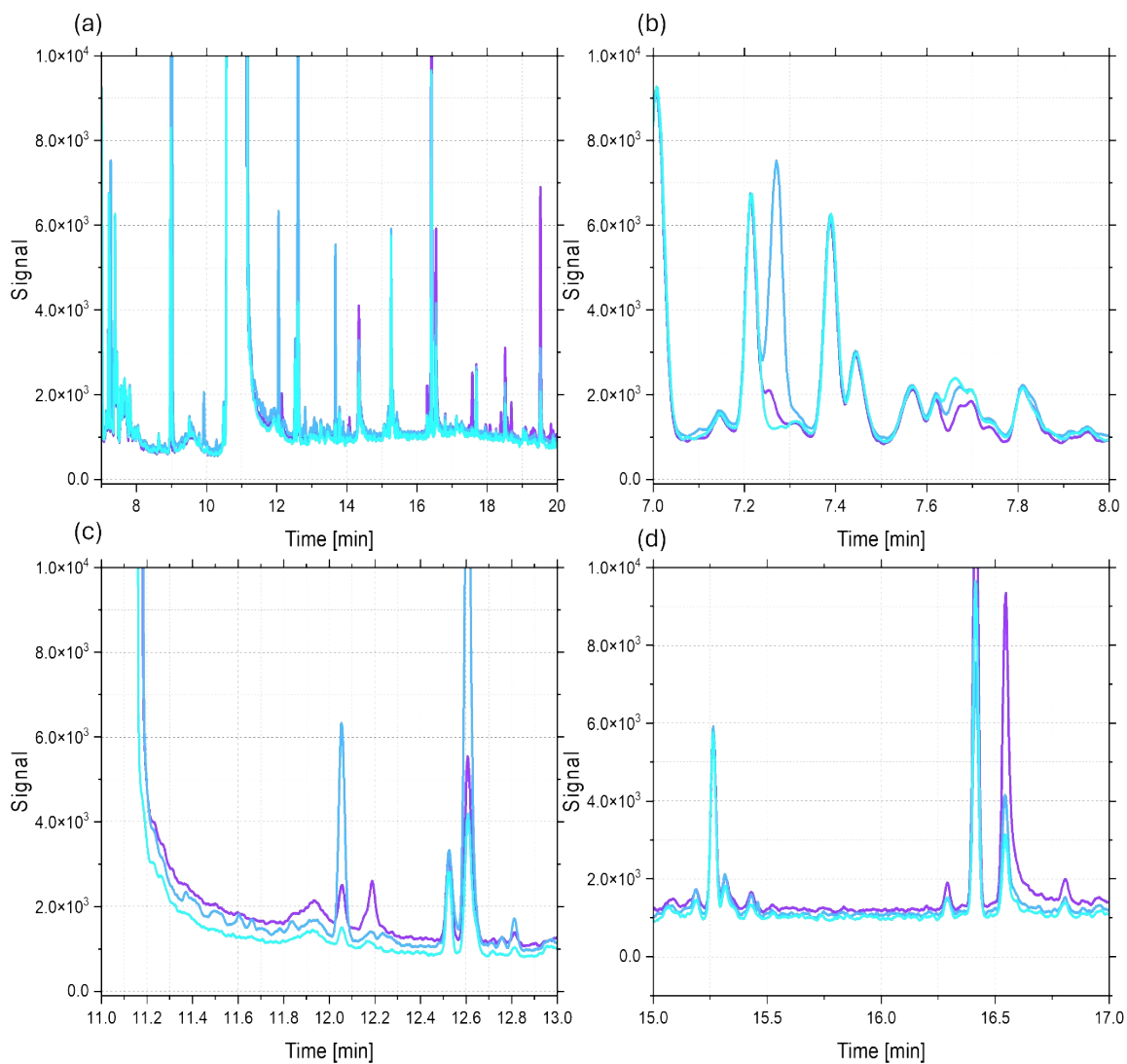


Fig. S12 GC-MS characterization of the distillation of an artificially wetted solvent. The chromatograms of the feed (violet, acquired after the distillation) and two subsequent distillates are shown (blue and turquoise). The first few milliliters of the distillate were discarded. Then, approximately 10 milliliters were collected as distillate 1 (turquoise). The distillation distribution adapter was then switched to the next flask to collect a further 30 milliliters as distillate 2 (blue). Again the main 7A peak was cut off to highlight the impurity peaks. (a) overview and (b)-(d) close-ups of selected retention time regions. All three spectra are qualitatively similar. While some impurities could be reduced by distillation (e.g. the peak at a retention time of 16.6 min), others were enriched in distillate 1 and then reduced in distillate 2 (e.g. the peak at a retention time of 12.6 min). In summary, vacuum distillation was ineffective at removing the impurities identified by GC-MS. These experiments suggest that distilling wet 7A may introduce new impurities through chemical reactions with water.

Details of solvent treatments

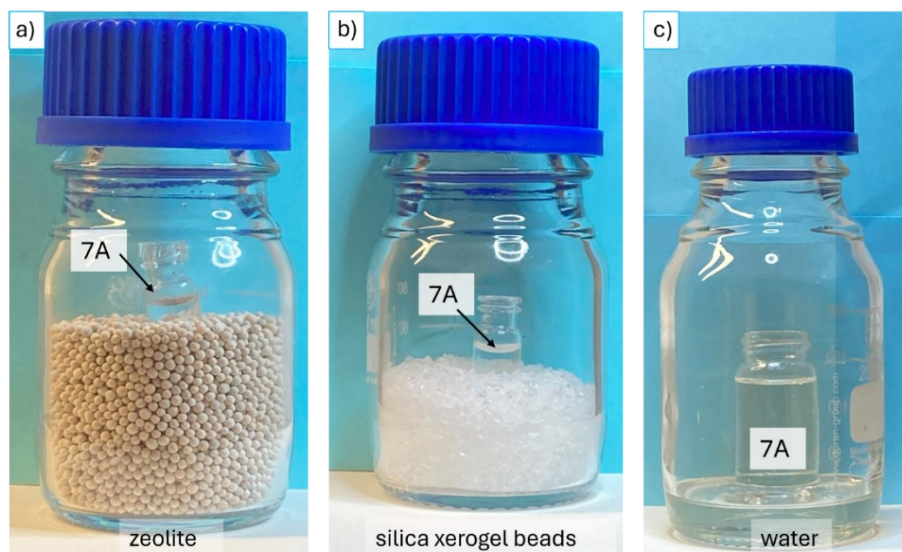


Fig. S13 Photographs showing the experimental setups for drying the 7A solvent with (a) 3A zeolite and (b) silica xerogel beads in the container and (c) wetting the 7A solvent with water vapor. In the first two cases, a small vial (2 mL) containing 7A solvent or TMA solution was placed in a larger laboratory flask (100 mL) containing a large amount of either (a) 3A zeolite or (b) silica xerogel beads. For solvent wetting, a small vial (20 mL) containing 7A solvent was placed in a larger laboratory flask (100 mL) containing liquid water at the bottom. For thermal treatment, the containers were tightly sealed and placed in a ventilated laboratory oven.

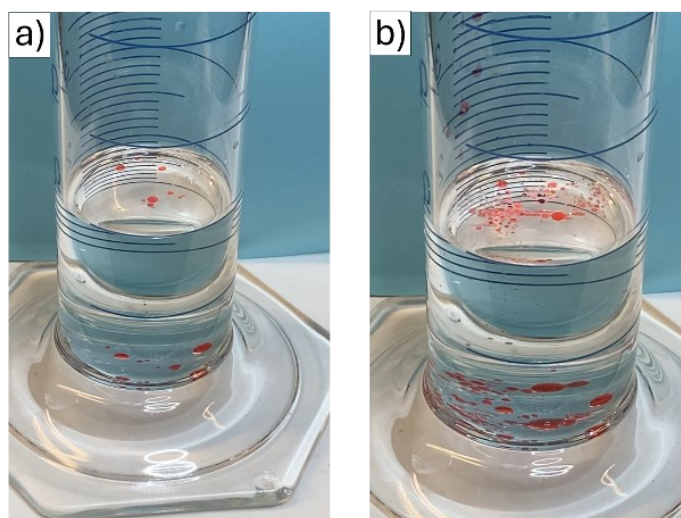


Fig. S14 Photographs showing the water droplets that formed after adding (a) 10 mmol/L and (b) 100 mmol/L of liquid water to pure 7A solvent. The larger droplets sank to the bottom and formed a sediment, while the smaller ones floated. Homogenization was achieved by sonicating the wetted 7A solvents at elevated temperatures. To enhance the contrast between the two substances in this illustration, the water was stained with amaranth (trisodium (4E)-3-oxo-4-[(4-sulfonate-1-naphthyl)hydrazono]naphthalene-2,7-disulfonate), an organic dye that is highly soluble in water but virtually insoluble in 7A.

References

1. J. M. Soler, E. Artacho, J. D. Gale, A. García, J. Junquera, P. Ordejón and D. Sánchez-Portal, *J. Phys.-Condens. Mat.*, 2002, **14**, 2745-2779.
2. A. García, N. Papior, A. Akhtar, E. Artacho, V. Blum, E. Bosoni, P. Brandimarte, M. Brandbyge, J. I. Cerda, F. Corsetti, R. Cuadrado, V. Dikan, J. Ferrer, J. Gale, P. García-Fernández, V. M. García-Suárez, S. García, G. Huhs, S. Illera, R. Korytár, P. Koval, I. Lebedeva, L. Lin, P. López-Tarifa, S. G. Mayo, S. Mohr, P. Ordejón, A. Postnikov, Y. Pouillon, M. Pruneda, R. Robles, D. Sánchez-Portal, J. M. Soler, R. Ullah, V. W. Z. Yu and J. Junquera, *J. Chem. Phys.*, 2020, **152**.
3. J. P. Perdew, K. Burke and M. Ernzerhof, *Phys. Rev. Lett.*, 1996, **77**, 3865-3868.
4. S. Grimme, *J. Comput. Chem.*, 2006, **27**, 1787-1799.
5. M. Lackinger, S. Griessl, W. M. Heckl, M. Hietschold and G. W. Flynn, *Langmuir*, 2005, **21**, 4984-4988.